

Technical Notes

TECHNICAL NOTES are short manuscripts describing new developments or important results of a preliminary nature. These Notes cannot exceed 6 manuscript pages and 5 figures; a page of text may be substituted for a figure and vice versa. After informal review by the editors, they may be published within a few months of the date of receipt. Style requirements are the same as for regular contributions (see inside back cover).

Dynamic Instability Caused by Forebody Blowing

LARS E. ERICSSON* AND ROLF A. GUENTHER†
Lockheed Missiles and Space Company Inc., Sunnyvale, Calif.

THE nose-heavy distributed blowing used by Stalmach et al.¹ to obtain the data in Fig. 1 will induce bow shock curvature. Nose bluntness also induces a curved bow shock, and it has been shown that the associated entropy wake is responsible for the experimentally observed trends, i.e., increasing static but decreasing dynamic stability for moderate nose bluntness.² Comparing the zero amplitude ($\Delta \dot{m} = 0$) blowing data in Fig. 1 with the nose bluntness effects does not leave much doubt about the similarity (Fig. 2);[‡] that is, increasing mean blowing rate has an effect similar to increasing the nose bluntness. There is one important difference, however; the increased blowing leads to negative pitch damping which pure nose bluntness cannot produce. A difference in c.g. locations, e.g., $x_{CG}/l = 0.671$ compared to $x_{CG}/l = 0.600$, affects the nose bluntness-induced degradation of the dynamic stability derivative very little, although it has a dominant effect on the change of static stability as shown in Fig. 9 of Ref. 1 and Fig. 8 of Ref. 3.

It has been shown by Syvertson and McDevitt⁴ that the nose blowing effects are very similar to the effects of hammerheaded spherical nose bluntness. As the entropy gradients behind a sphere, e.g., on a hemisphere-cylinder body,⁵ are much steeper than over the conical frustum of a blunted cone,² the hammer-

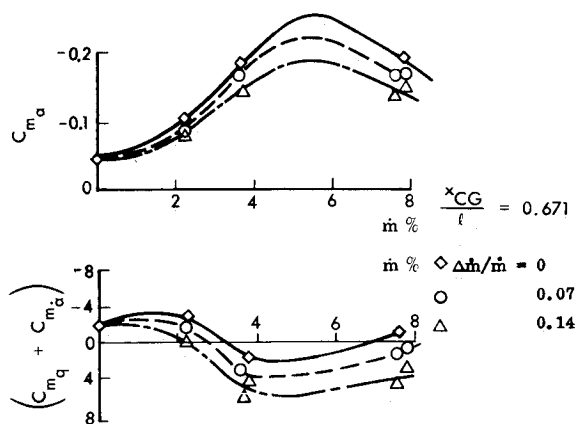


Fig. 1 Effect of blowing on the static and dynamic stability of a sharp 10° cone; $M = 17$, $\alpha = 0$, $\Delta \alpha = 1^\circ$.

Presented as Paper 72-31 at the AIAA 10th Aerospace Science Meeting, San Diego, Calif., January 17-19, 1972; submitted January 24, 1972; revision received September 25, 1972.

Index categories: Entry Vehicle Dynamics and Control; Nonsteady Aerodynamics; Supersonic and Hypersonic Flow.

* Senior Staff Engineer, Associate Fellow AIAA.

† Senior Aerodynamics Engineer.

‡ The scales of \dot{m} and d_N/d_B in Fig. 2 have not been related to each other analytically but were chosen only to indicate the qualitative similarity.

□ SYMBOLS INDICATE DATA THAT HAVE BEEN CORRECTED FOR BREATHING EFFECTS AT $\dot{m} = 0$

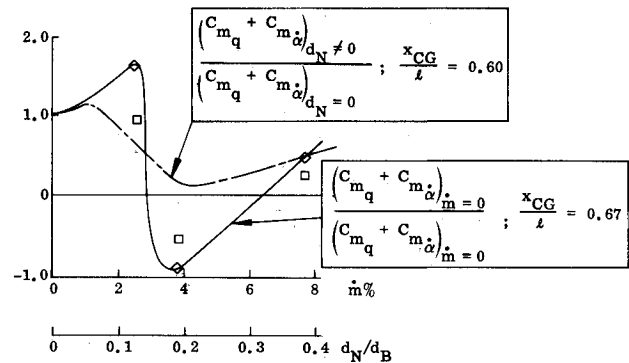


Fig. 2 Comparison between effects of blowing and nose bluntness on the pitch damping of 10° cones.

headed nose bluntness should produce a larger dynamically destabilizing effect than regular nose bluntness. The hammerhead geometry is represented by the hemisphere-cylinder-cone geometry shown in Fig. 3. The cylinder is simply the surface of the hypersonic shadow cast by the spherical nose. Combining the results for cylinder-flare bodies⁵ with the results for blunted cones,² one can approximate the bow shock shape as shown in Fig. 3. It has been shown earlier^{2,5} that the bow shock-generated entropy wake has similar profiles which can be described by a similarity parameter χ^* , defined by the relative distance radially from the surface element to the bow shock.

For a spherically blunted cylinder, the inner portion of the entropy wake has a dynamic pressure distribution that can be described as follows⁵

$$\rho U^2 / \rho_\infty U_\infty^2 = f^*(\chi_C^*) = 0.165 + 2.75 \chi_C^* \quad (1)$$

The corresponding expression for the blunted conical frustum is²

$$\rho U^2 / \rho_\infty U_\infty^2 = f^*(\chi_F^*) = 0.165 + (2.75/2) \chi_F^* \quad (2)$$

That is, the shock radius is larger in the case of the blunted cone by a factor of $2^{1/2}$.

With the coordinate system defined in Fig. 3, the shock radius for the sphere-cylinder is defined as follows⁶

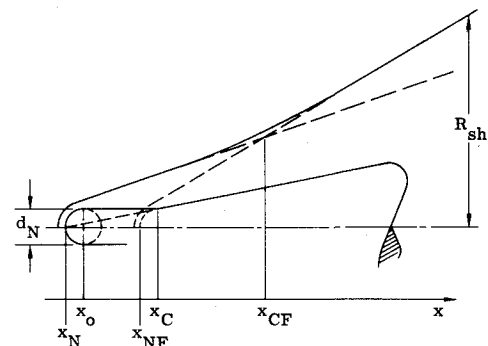


Fig. 3 Definition of compound sphere-cylinder-cone geometry.

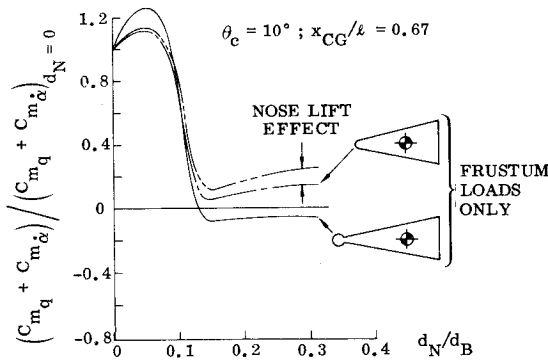


Fig. 4 Comparison between hemispherical and spherical nose tip effects.

$$(R_{sh}/d_N)^2 = C_{D_N}^{1/2}(x/d_N - x_N/d_N) \quad (3)$$

where $x_N/d_N = -\frac{1}{2}$. The shock radius for the conical frustum is

$$(R_{sh}/d_N)^2 = 2C_{D_N}^{1/2}(x/d_N - x_C/d_N - x_N/d_N) \quad (4)$$

The two shock radii coincide at x_{CF}

$$x_{CF}/d_N = 2(x_C/d_N) - x_N/d_N \quad (5)$$

Equation (3) gives the following definition for $f = 2f^*$ of the hemisphere-cylinder-cone geometry (Fig. 3)

$$f = \begin{cases} 0.33 + 5.5\chi^* & \chi^* < 0.2945 \\ 2.00 & \chi^* \geq 0.2945 \end{cases} \quad (6)$$

The parameter χ^* is determined by modifying earlier analysis^{2,5} as follows: when $x/d_N \leq x_{CF}/d_N$, the shock radius is defined by Eq. (3). When $x/d_N > x_{CF}/d_N$, the cylinder wake profile is stretched to the conical shock, the radius of which is defined by Eq. (4). The coordinate x_C is $x_C/d_N = 0.5 \cot \theta_c$ for $\alpha = 0$, and is obtained simply for $\alpha \neq 0$ using the tangent cone approximation.[§]

Incorporating these modifications in the embedded Newtonian computer program for regular blunt noses² gives the following results: the oversize spherical nose bluntness does produce negative pitch damping (Fig. 4), but does not explain the full effect of nose blowing (compare Figs. 2 and 4). Re-examining the blowing data in Fig. 1, especially the $\Delta \dot{m} = 0$ data (obtained by extrapolation from the data for $\Delta \dot{m}/\dot{m} = 0.07$ and 0.14), one finds the data for small \dot{m} suspicious. Eckstrom⁷ found that the porous skin allowed breathing at $\dot{m} = 0$, causing a reduction of C_{N_z} . Similar results have been observed by Wimberly et al.,⁸ who found the reduction of C_{N_z} to be 20% for a 7.25° cone. This would correspond to a 42% reduction for a 10° cone, assuming that the breathing action increases linearly with frustum cone angle. Correcting the $\Delta \dot{m} = 0$ data of Stalmach et al. for this 42% reduction at $\dot{m} = 0$, gives the data shown in Fig. 2 with a square symbol.[¶] It can be seen that the low \dot{m} -trend now looks more reasonable, although the spherical nose bluntness still produces only a portion of the experimentally observed undamping due to blowing. Something is missing.

So far no consideration has been given to the effect of crossflow on the blowing. It has been shown before that the effect of aft body nonphased blowing is damping (and slightly destabilizing statically),^{9,10} and cannot explain the negative damping measured by Stalmach et al. However, if one considers the crossflow effects near the nose, it is obvious that they can cause a displacement of the bow shock with associated change of entropy wake on the leeward side. Locally this shock displacement would cause increased pressure, resulting in decreased nose lift. Such an effect has been observed for boundary-layer crossflow at moder-

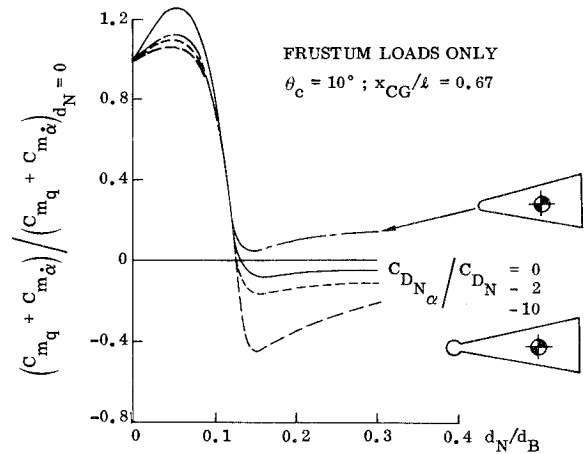


Fig. 5 Comparison between effects of hemispherical, spherical, and attitude-sensitive spherical nose tip effects on pitch damping.

ately high angles of attack.¹¹ It is conceivable that the crossflow effect could be much stronger for a boundary layer with mass addition and could provide an effective increase of the leeward-side blowing-induced apparent nose bluntness already at small angles of attack. The resultant effect is that the apparent nose bluntness is larger on the leeward side, causing a more displaced bow shock than on the windward side. This is exactly the opposite of the deviation caused by a conical nose tip.¹² Representing this effect by an imaginary conical nose tip with $C_{D_{Nz}} = -C_{D_{Nz}}(\theta_N)$ (i.e., with the same magnitude as a conical nose tip but of opposite sign) gives the results shown in Fig. 5. Comparing Figs. 2, 4, and 5, one can see that attitude-sensitive nose bluntness can explain the measured negative damping, although the magnitude of this nose attitude effect has to be substantially larger than that of a conical tip. $|C_{D_{Nz}}/C_{D_N}| = 2$ is the maximum value for a conical tip. Reference 1 also contains data for nose blowing (Fig. 6). The blowing rates $\dot{m}_N > 3.5\%$ may well be outside of the range of boundary-layer blowing discussed here; i.e., they cause boundary-layer blowoff and generation of an inner shear layer which has to be added to the "entropy wake."

The effects of nose bluntness and blowing have been presented as the (fractional) change of the stability derivatives for a cone with zero nose bluntness and zero blowing, respectively. In this manner those boundary-layer crossflow and sting-interference effects that are the same for both sharp and blunt cones were eliminated from the comparison between nose bluntness effects, as indicated by inviscid theory and measured in viscous experi-

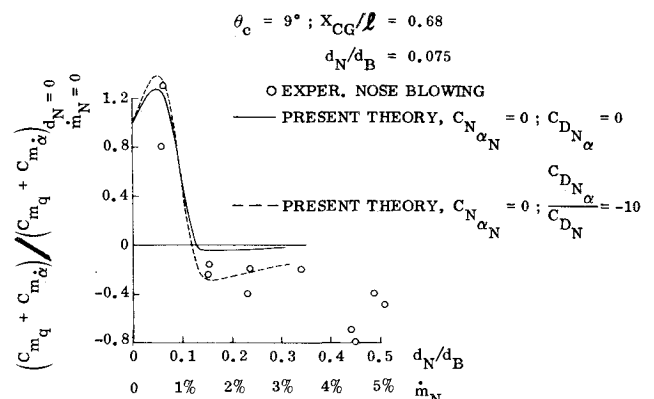


Fig. 6 Comparison between effect of spherical nose tip and nose blowing.

§ And assuming that the intersection between the nose shadow and the conical frustum can be approximated by the intersection made by a plane through top and bottom intersection points.

¶ This brings the data point for $\dot{m} = 0$ in Fig. 1 into excellent agreement with inviscid theory.

ments.^{2**} In regard to the sting interference, there was some doubt that the nose-bluntness-induced entropy-swallowing effects would really be negligible when they occurred near the base.¹⁴ The effects of forebody blowing, which include both apparent nose bluntness and boundary-layer thickening effects, are even more unlikely to be negligible. That is, one can expect the sting interference to increase with the blowing rate. In a hypersonic test the sting interference is usually of the sting-flare type, causing a degradation of dynamic stability.¹⁴ Thus, one could suspect that sting interference was responsible for part of the negative damping effect of forebody blowing measured by Stalmach et al.¹ Fortunately, the sting used in the test had the flared strut fairing more than 4 base diameters downstream of the base,¹⁵ and dynamic sting interference is not likely to have distorted the data trends measured by Stalmach et al.

The following conclusions can be drawn from an analysis of the effects of forebody blowing on the unsteady aerodynamics of slender cones: Forebody blowing has a dynamically destabilizing effect which can produce negative pitch damping at moderately high blowing rates. The experimentally observed undamping effect of forebody blowing can be simulated qualitatively by an apparent nose bluntness. It remains to be determined how the bow shock curvature varies with the blowing rate before a quantitative prediction of the blowing effect can be made.

References

- ¹ Stalmach, C. J., Jr., Lindsey, J. L., and Pope, T. C., "Hypersonic Aerodynamic Measurements on a 10° Cone with Oscillatory Mass Addition," AIAA Paper 70-217, New York, Jan. 1970.
- ² Ericsson, L. E., "Effects of Nose Bluntness, Angle of Attack, and Oscillation Amplitude on Hypersonic Unsteady Aerodynamics of Slender Cones," *AIAA Journal*, Vol. 9, No. 2, Feb. 1971, pp. 297-304.
- ³ Ericsson, L. E., "Universal Scaling Laws for Hypersonic Nose Bluntness Effects," *AIAA Journal*, Vol. 7, No. 12, Dec. 1969, pp. 2222-2227.
- ⁴ Ericsson, L. E., "Effects are Negligible at Hypersonic Speeds—Fact or Fiction?," *Transactions of the 19th Congress of the International Astronautical Federation*, Vol. 3, *Propulsion Reentry Physics*, Pergamon Press, PWN—Polish Scientific Publishers, New York, Oct. 1968, pp. 547-561.
- ⁵ Ericsson, L. E., "Unsteady Aerodynamics of an Ablating Flared Body of Revolution Including Effect of Entropy Gradient," *AIAA Journal*, Vol. 6, No. 12, Dec. 1968, pp. 2395-2401.
- ⁶ Sieff, A. and Whiting, E. E., "A Correlation Study of the Bow-Wave Profiles of Blunt Bodies," TN D-1148, 1962, NASA.
- ⁷ Eckstrom, D. J., "The Influence of Mass and Momentum Transfer on the Static Stability and Drag of a Slender Cone—An Experimental Correlation," LMSC/D051269, July 1968, Lockheed Missiles & Space Co., Sunnyvale, Calif.
- ⁸ Wimberly, C. R., McGinnis, F. K., III, and Bertin, J. J., "Transpiration and Film Cooling Effects for a Slender Cone in Hypersonic Flow," *AIAA Journal*, Vol. 8, No. 6, June 1970, pp. 1032-1038.
- ⁹ Ericsson, L. E. and Reding, J. P., "Ablation Effects on Vehicle Dynamics," *Journal of Spacecraft and Rockets*, Vol. 3, No. 10, Oct. 1966, pp. 1476-1483.
- ¹⁰ Ericsson, L. E., "Effect of Boundary Layer Transition on Vehicle Dynamics," *Journal of Spacecraft and Rockets*, Vol. 6, No. 12, Dec. 1969, pp. 1390-1396.
- ¹¹ Friberg, E. G. and Walchner, O., "Pressure Correlation for Blunted Slender Cones," *AIAA Journal*, Vol. 7, No. 8, Aug. 1969, pp. 1618, 1619.
- ¹² Ericsson, L. E. and Guenther, R. A., "Effect on Slender Vehicle Dynamics of Change from Spherical to Conical Nose Bluntness," *Journal of Spacecraft and Rockets*, Vol. 9, No. 6, June 1972, pp. 435-440.
- ¹³ Brong, E. A., "The Unsteady Flow Field About a Right Circular Cone in Unsteady Flight," FDL-TDR-64-148, Jan. 1967, Air Force Flight Dynamics Lab., Wright-Patterson Air Force Base, Ohio.
- ¹⁴ Reding, J. P. and Ericsson, L. E., "Dynamic Support Interference," *Journal of Spacecraft and Rockets*, Vol. 9, No. 7, July 1972, pp. 547-553.
- ¹⁵ Stalmach, C. J., Jr., private communication, Feb. 1972, Sunnyvale, Calif.

Experimental Investigation of Two-Dimensional, Supersonic Flow Impingement on a Normal Surface

CHARLES V. KNIGHT*

University of Tennessee at Nashville, Nashville, Tenn.

Nomenclature

- D = exit dimension of nozzle
 S = finite distance ahead of normal surface
 SD = standoff distance ahead of normal surface
 X = distance from center of normal surface
 Y = distance from nozzle exit plane

Introduction

MOST studies of jet impingement have been of the subsonic, axisymmetric jet variety.¹⁻⁴ Rudov and Uskov⁵ and others have investigated the effect of flow impingement on inclined barriers as might result from supersonic jet engine nozzles. No data are available for a finite-size, axisymmetric, supersonic flow impingement on a surface normal to the nozzle centerline in the presence of the atmosphere.

Shauer and Eustis⁶ in 1963 conducted an experimental and theoretical investigation of subsonic, two-dimensional jet impingement flows. Wolfshtein⁷ and others have used the data of Shauer and Eustis in testing complex mathematical models of jet impingement flows.

In this experimental investigation data on the impingement are presented for the specific case of two-dimensional, supersonic jet flow. These experimental data are significant first because of their unique dependence on the effects of compressibility and secondly due to the fact that these data may be used to test future mathematical models related to impingement. Previously the testing of such compressible models relied on the use of oversimplified incompressible experimental data.

Description of the Experiment

The supersonic flow for use in the investigation was produced by a continuous flow, fully expanded nozzle designed for a Mach number of 1.9 (experimentally delivering $M = 1.89$). The exit dimensions of the nozzle are 1×0.464 in. while the throat is 1×0.3 in. For the experimental investigation, the stagnation temperature was maintained at 75°F, and the stagnation pressure was set at 95.3 psia. This resulted in a nozzle exit Reynolds number of 822,000 where the Reynolds number was based on the significant nozzle dimension of 0.464 in.

The insert in Fig. 1 presents a schematic of the flowfield and associated apparatus used in this investigation. The normal surface was designed such that it could be traversed from the nozzle exit to 15 in. downstream of the nozzle exit. Regions of flow development (I), developed flow (II), and stand-off (III) are shown in the insert in Fig. 1 to illustrate their basic distinction. For normal surface positions very close to the nozzle the developed flow region does not exist. Some very significant data resulting from such close nozzle-to-normal-surface positions are presented.

Received March 4, 1972; revision received July 12, 1972.

Index categories: Nozzle and Channel Flow; Jets, Wakes, and Viscid-Inviscid Flow Interactions.

* Assistant Professor, Division of Engineering, Associate Member AIAA.

** The inviscid sharp cone data as defined by Newtonian theory can be obtained from Ref. 2 by setting $f = 2$ and $g = 1$. For a more accurate value the numerical methods of Ref. 13 can be used.